Inhibition of Class C β-Lactamases: Structure of a Reaction Intermediate with a Cephem Sulfone[†,‡]

Gregg V. Crichlow,[§] Michiyoshi Nukaga,[§] Venkata R. Doppalapudi,[||] John D. Buynak,[||] and James R. Knox*[,§]

Department of Molecular and Cell Biology, The University of Connecticut, Storrs, Connecticut 06269-3125, and Department of Chemistry, Southern Methodist University, Dallas, Texas 75275-0314

Received January 22, 2001; Revised Manuscript Received April 5, 2001

ABSTRACT: The crystallographic structure of the *Enterobacter cloacae* GC1 extended-spectrum class C β-lactamase, inhibited by a new 7-alkylidenecephalosporin sulfone, has been determined by X-ray diffraction at 100 K to a resolution of 1.6 Å. The crystal structure was solved by molecular replacement using the unliganded structure [Crichlow et al. (1999) *Biochemistry 38*, 10256−10261] and refined to a crystallographic *R*-factor equal to 0.183 (R_{free} 0.208). Cryoquenching of the reaction of the sulfone with the enzyme produced an intermediate that is covalently bound via Ser64. After acylation of the β-lactam ring, the dihydrothiazine dioxide ring opened with departure of the sulfinate. Nucleophilic attack of a side chain pyridine nitrogen atom on the C6 atom of the resultant imine yielded a bicyclic aromatic system which helps to stabilize the acyl enzyme to hydrolysis. A structural assist to this resonance stabilization is the positioning of the anionic sulfinate group between the probable catalytic base (Tyr150) and the acyl ester bond so as to block the approach of a potentially deacylating water molecule. Comparison of the liganded and unliganded protein structures showed that a major movement (up to 7 Å) and refolding of part of the Ω-loop (215−224) accompanies the binding of the inhibitor. This conformational flexibility in the Ω-loop may form the basis of an extended-spectrum activity of class C β-lactamases against modern cephalosporins.

The primary cause of bacterial resistance to penicillins and cephalosporins is the action of β-lactamase enzymes, which hydrolytically destroy β-lactam antibiotics (*1*, *2*). Of the four classes in which the enzymes are grouped, class B β-lactamases are metalloenzymes while classes A, C, and D are serine enzymes which have mechanisms involving nucleophilic attack of the reactive serine on the carbon of the β-lactam amide. A similar mechanism is found in the enzyme targets of the β-lactams, D-alanine-D-alanine carboxypeptidases/transpeptidases, which are instrumental in cell wall synthesis (*3*−*5*). The deacylation of the acyl intermediate in the target enzymes is very slow and leads to long-term inactivation and cell death, whereas deacylation of the intermediate is much faster in the β-lactamases, causing rapid turnover of β-lactams and protection of the cell (*6*).

Clinically, class A and C β-lactamases are the most commonly encountered. Plasmid-mediated class A β-lactamases are widely distributed in both Gram-negative and Gram-positive organisms. Class C enzymes, such as AmpC, are mainly chromosomal and are typically synthesized by Gram-negative organisms (*7*). Through the 1990s, approximately one or two new plasmid-encoded AmpC β-lactamases have been discovered annually, so that class C β-lactamases, including both chromosomal and plasmid-borne enzymes, are now present in 10−50% of patients infected with *Citrobacter freundii, Enterobacter cloacae*, *Serratia marcescens*, and *Pseudomonas aeruginosa* (*8*).

One strategy for overcoming β-lactamase-mediated resistance is to design antibiotics which are poor β-lactamase substrates. Thus appeared in the 1980s the third generation cephalosporins, such as ceftazidime, which incorporate bulky oxyimino substituents on the C7 side chain. However, these have fallen susceptible to extended-spectrum β-lactamases (ESBL's), which are typically plasmid-mediated class A enzymes that are able to accommodate the oxyimino substituent (*9*). Moreover, a chromosomal class C ESBL has been isolated from the Gram-negative *E. cloacae* strain GC1 (*10*). The GC1 β-lactamase is very similar in both sequence and overall structure to the enzyme of *E. cloacae* P99, the parental strain which does not have extended-spectrum activity (*7*, *11*). The improved performance by GC1 is apparently due to a peptide insertion consisting of an unusual tandem repeat of three residues in a disordered region of the protein called the Ω-loop (*12*, *13*).

Another approach to combat resistance is the coadministration of a β-lactam antibiotic and a β-lactamase inhibitor (*14*, *15*). Inhibitors that are presently available (such as clavulanic acid, sulbactam, and tazobactam) are generally effective against the class A enzymes, but their usefulness is rapidly declining with the appearance of mutant forms, and they display little inhibition of the class C enzymes, which are of increasing clinical signifcance. To identify inhibitors capable of inactivating both class A and class C β-lactamases, structure−activity relationships have been

[†] J.D.B. thanks the Robert A. Welch Foundation for continued support.

[‡] Atomic coordinates have been deposited in the Protein Data Bank (entry 1GA0) at Rutgers University.

* Corresponding author: phone 860-486-3133; fax 860-486-4745; e-mail knox@uconnvm.uconn.edu.

[§] The University of Connecticut.

[||] Southern Methodist University.

10.1021/bi010131s CCC: $20.00
Published on Web 05/04/2001

explored in both the 6-alkylidenepenicillin sulfone (**1**) (*16*−*18*) and the 7-alkylidenecephalosporin sulfone (**2**) (*19*) series,

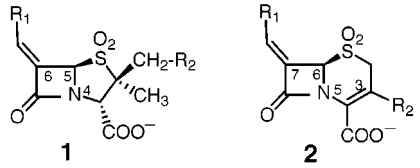

where broad-spectrum inactivators have been identified (*20*). The sulfone DVR-II-41S (**3**) has been found to inhibit the class A enzymes TEM-1 and PC1 as well as the P99 and GC1 class C enzymes (*21*). For optimization of design, it is desirable to learn the binding interactions and reaction mechanism of such inhibitors that incorporate both a sulfone and a 7-position alkylidene unit in a cephalosporin skeleton (*22*). Here we present the structure of the class C GC1 β-lactamase after its reaction with sulfone **3**.

MATERIALS AND METHODS

Subcloning and Protein Purification. The enzyme was obtained from the GC1 β-lactamase gene on the pCS101 plasmid in *Escherichia coli* AS226-51, as previously described (*13*, *23*).

Synthesis and Purification of Inhibitor. Compound DVR-II-41S (**3**) was prepared as reported (*19*). The sodium salt was purified by chromatography on Diaion CHP20P (Mitsuibishi Chemical Corp., White Plains, NY) and judged to be at least 95% pure by NMR.

Crystallization of the Native Protein. The β-lactamase from *E. cloacae* GC1 was crystallized using the sitting drop vapor diffusion method from a drop containing 5.6% PEG[1] (M_r = 3350) and 9.1 mM imidazole, pH 7.0, over a reservoir of 24% PEG (low ionic strength screen; Hampton Research). The native crystals had platelike morphology and unit cell parameters a = 78.0 Å, b = 69.5 Å, and c = 63.1 Å in orthorhombic space group $P2_12_12$ with one monomer in the asymmetric unit.

Reaction with Inhibitor. A representative crystal of approximate dimensions 0.20 mm × 0.17 mm × 0.025 mm was soaked in a solution of 9 mM **3**, 15 mM imidazole, and 28% PEG 3350 at pH 7.0 for 3 h. It then was soaked in a fresh, identical solution for 35 min, after which time the crystal was soaked in 20 mM HEPES, 24% PEG, and 25% glycerol for 2 min to prevent ice crystal formation upon cryocooling.

X-ray Data Collection. A loop-mounted crystal was flash cooled and kept at 100 K with nitrogen gas (Oxford Cryosystems). One degree oscillation data were collected on a Quantum 4 CCD detector (Area Detector Systems Corp.) at station A1 of the Cornell High Energy Synchrotron Source (MacCHESS). All data were collected from one crystal.

Data Reduction. Examination of the intensities confirmed Laue symmetry *mmm* and space group $P2_12_12$, as in the native crystals. The reacted crystal had cell dimensions a = 77.0 Å, b = 69.0 Å, and c = 62.5 Å, representing a 2.9% decrease in unit cell volume relative to the native crystal. The HKL data reduction package (*24*) was used to reduce 103° of data containing 94 739 observations of 29 788 unique reflections from 50 to 1.6 Å resolution (Table 1). The R_{merge}-(based on I) is 8.7%.

Table 1: X-ray Data Collection[a]

temp (K)	100
d_{min} (Å)	1.6 (2.02−1.6)
observations	94739 (12241)
unique reflections	29788 (7159)
completeness	0.661 (0.322)
av $I/\sigma(I)$	7.8 (2.7)
$R_{sym}(I)$[b]	0.087 (0.31)

[a] Data for highest resolution shell are in parentheses. [b] $R_{sym} = \sum|I_{av} - I_i|/\sum I_i$, where I_{av} is the average of all individual observations, I_i. The space group is $P2_12_12$.

RESULTS

Structure Determination. A molecular replacement search was carried out with the program AMoRe (*25*) using a model of the unliganded GC1 structure (1GCE). Water molecules were removed and three glycines inserted in place of residues 213−215 which could not be traced in the GC1 structure (*13*). The rotation function yielded a single solution with a correlation coefficient of 28% using an integration radius of 27 Å with resolution limits of 8−4 Å. A translation search improved the correlation to 68% and gave a crystallographic R-factor equal to 35%. After rigid body refinement the correlation coefficient and R-factor improved to 73% and 31%. The resulting model was generated using LSQKAB (*26*).

Map Fitting and Refinement of the Protein Model. Crystallographic refinement was done using X-PLOR (*27*), first from 8 to 2 Å and then to 1.6 Å resolution. Omit maps were calculated which excluded part of the Ω-loop (212−219) and the single turn of helix following it (220−224), as these segments were not completely traceable at this stage. The simulated annealing protocol was used for the early rounds of refinement with 2 Å data having $F > 2\sigma(F)$ and with a starting temperature of 1500 K. In later rounds of refinement, all data were included and various annealing temperatures used as well as nonannealing protocols.

Cross-validation using R_{free} (*28*) was used throughout the refinement. CHAIN (*29*) was employed for structure and map displays and for manual manipulation of the structure. Initial maps revealed significant but choppy electron density in the binding site, including density continuous with the reactive Ser64 side chain. The positions of Ser64 and Tyr150 were altered from their native positions, and residues 213−215, originally modeled as glycines, were converted to the true sequence (Arg-Val-Ser). Six residues were modeled in two conformations, including Thr319, a residue near the active site. After addition of water molecules and B-factor refinement, R decreased to 0.222 (R_{free} 0.263) without including the inhibitor in the model.

The density along the Ω-loop gradually improved when water molecules and a model of the intermediate were added (see below). Incorporation of a bulk solvent correction and map calculations omitting residues 220−224 of the single turn helix revealed a significant change in the path of this helix relative to the unliganded structure. Rigid body refinement of this segment was performed, and simulated annealing omit maps were used for the final fitting.

[1] Abbreviations: PEG, poly(ethylene glycol); rmsd, root of the mean of the squared deviations.

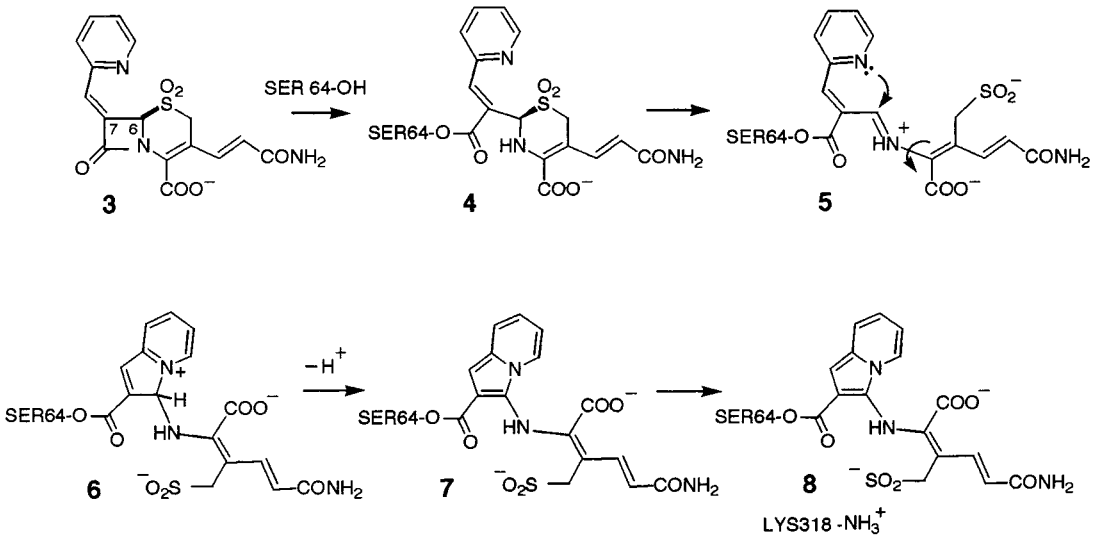

FIGURE 1: Scheme for the reaction of DVR-II-41S (**3**) with the reactive Ser64 of the GC1 β-lactamase. Adapted from ref *21*.

Table 2: Crystallographic Refinement

resolution range (Å)	100−1.6
no. of reflections used [$F > 0\sigma(F)$]	28503
R-factor	0.183
R_{free}-factor	0.208
residues in Ramachandran zones (%)	
favored	92.8
allowed	7.2
disallowed	0.0
rms deviations from ideality	
bond lengths (Å)	0.009
bond angles (deg)	1.5
planarity (deg)	1.0
mean *B*-factors (Å^2)	
protein	12.9
intermediate	42.5
water molecules	27.5
all atoms	14.7

Fitting and Refinement of the Intermediate. A model of a Ser64-bound reaction intermediate having both the β-lactam and dihydrothiazine rings open was fit to the improved density in the binding site. After preliminary refinement, the density strongly indicated that the intermediate contained a five-membered ring fused to the pyridine ring extending from C7. This new ring presumably formed by nucleophilic attack of the ring nitrogen on carbon C6 (Figure 1). The fused ring intermediate **8** was used in the final model and was refined with full occupancy. No restraints were applied to torsion angle rotations. For the sulfinic side chain two rotomers were used, differing by a 180° rotation about the $CH_2-SO_2^-$ bond.

The final cycles of refinement were performed with CNS (*30*) using all $F > 0\sigma(F)$ data (Table 2). A model of 363 residues from 2 to 364, the intermediate **8**, one molecule of glycerol near residues 245−248, a sodium ion near Glu124, and 315 water molecules ($B < 60$ Å^2) yielded an *R*-factor of 0.183 and R_{free} of 0.208. Ramachandran analysis showed 92.8% of the residues in most favored regions, with none disallowed. Two conformations were modeled for the side chains of Glu5, Asp248, Val294, Glu303, Thr319, and Val329. The oxygen and nitrogen atoms of the Gln120 side chain are disordered and omitted. Final maps of the electron density of reaction intermediate **8** and of the Ω-loop below it are shown in Figure 2. The mixed α/β tertiary structure is pictured in Figure 3a. Atomic coordinates have been deposited in the Protein Data Bank (entry 1GA0).

DISCUSSION

Prior crystallographic analysis of the unliganded GC1 β-lactamase (*13*), a natural variant of the parental P99 enzyme, revealed disorder below the binding site, in the so-called Ω-loop (189−226). The disordered segment included part of an unusual tandem tripeptide insertion, with residues 213−215 invisible in the electron density map. The insertion moved the Ω-loop 1−2 Å away from the reactive Ser64 and appeared to enlarge the binding cavity for β-lactam entry. These findings supported the hypothesis that the three-residue insertion permits the enzyme to accommodate β-lactams with larger C7 substitutents. In addition, the larger cavity allows the acyl intermediate more conformational freedom, with increased hydrolysis. Here, in an acylated sulfone, we must explain a low rate of hydrolysis.

Comparison of the Liganded and Unliganded Enzymes. In contrast to the electron density map of the unliganded enzyme, the map of the inhibited enzyme clearly shows every residue in the Ω-loop (Figure 2b), indicating that the binding of the inhibitor has somehow reduced the flexibility of the Ω-loop. However, it is surprising that there is little direct contact between the Ω-loop and the intermediate. Perhaps an earlier intermediate in the reaction pathway (Figure 1) contacted the Ω-loop and induced in it a conformational change to the stable conformation we now see. An overlay of the liganded and unliganded structures shows that a likely point of contact could have been the side chain ring of Tyr224 (Figure 3b). It has been displaced 6 Å from its central position in the empty binding cavity to a more recessed position at the rear of the inhibitor-occupied cavity where its ring stacks with the side chain of Arg213.

The conformation of the Ω-loop is not only stabilized by the inhibition process but also altered considerably with respect to its conformation in the unliganded enzyme. The overlay of the two structures is rather close from the beginning of the Ω-loop to Val212, after which a significant refolding occurs from residue 216 through residue 224, with maximum shifts up to 7 Å and a more elongated conforma-

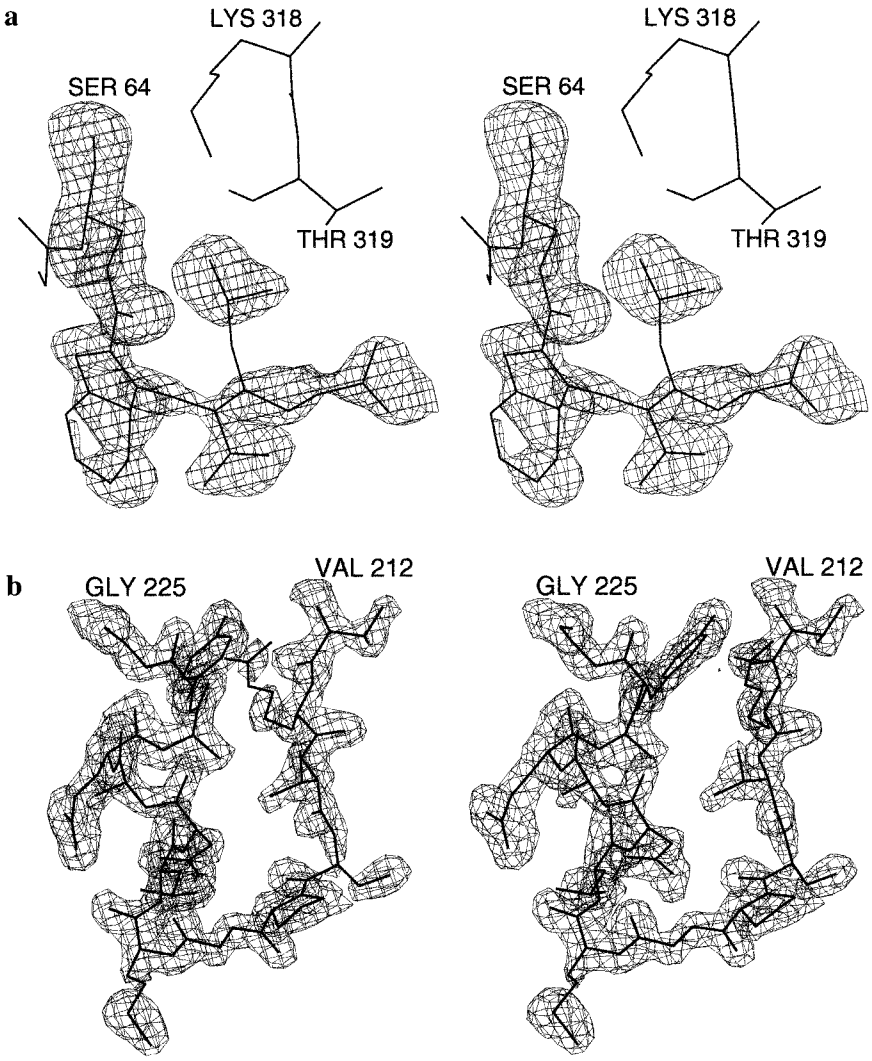

FIGURE 2: (a) Stereoview of the $F_o - F_c$ electron density map of the DVR-II intermediate **8** covalently bonded to Ser64. The intermediate and Ser64 were omitted from the F_c calculation. The contour level is 2.5σ. (b) Stereoview of the $2F_o - F_c$ map of the Ω-loop region from residues 212 to 225. The contour level is 1.0σ. The maps were plotted by CHAIN (*29*).

tion of the loop. At the end of the Ω-loop, the five-residue single turn α-helix (220−224) assumes an orientation more parallel to the middle section of the loop. The helix rolls 20−30° about it axis, carrying with it the Tyr224 mentioned above. After the liganded and unliganded structures were overlayed, the rmsd for all Cα positions is 0.85 Å but is only 0.24 Å if the 12 Ω-loop residues from Arg213 to Tyr224 are omitted.

Parenthetically, we note a recent discovery of a significant modification in the folding of the Ω-loop of a class A β-lactamase. The crystal structure of the (unliganded) PER-1 enzyme (*31*), having expanded activity against cephalosporins with bulky substituents, reveals that the absence of a normally conserved cis peptide bond in the Ω-loop results in a major alteration in the Ω-loop relative to other wild-type class A β-lactamases.

The change in the Ω-loop conformation of this class C enzyme is particularly interesting in light of the extended-spectrum activity, which was first detected in its ability to hydrolyze ceftazidime, a cephaloporin with a bulky C7 oxyimino side chain (*10*). Ceftazidime is not efficiently hydrolyzed by the wild-type P99 enzyme, which does not contain the three-residue insertion in the Ω-loop. Interestingly, the Ω-loop in the P99 enzyme does not undergo a conformational change in the presence of a phosphonate inhibitor (*32*). Therefore, in the GC1 mutant the movement of Ω-loop residue Tyr224 away from the binding site possibly reduces steric hindrance to the oxyimino side chain and may be the event that enhances hydrolysis of cephalosporins containing these large C7 side chains.

This diminished steric hindrance may have an effect on deacylation. Patera et al. (*33*) found in the acyl intermediate structure of cloxacillin with the class C *E. coli* AmpC β-lactamase that, due to steric hindrance with the enzyme, the large C6 side chain of this penicillin must fold back on itself, pushing the five-member penicillin ring upward toward the lysine (here Lys318) of the B3 strand. This ring movement positions the C3 carboxylic acid group where it blocks the approach of the deacylating water molecule, similar to the blocking by sulfinate described below. Cephalosporins with large oxyimino side chains may be resisting hydrolysis by the P99 and other non-ESBL class C β-lactamases in the same manner to decrease the deacylation rate. The observed shifting of Tyr224 in GC1 away from the binding site therefore creates a space where such a large side chain may fit in a more extended, less sterically strained

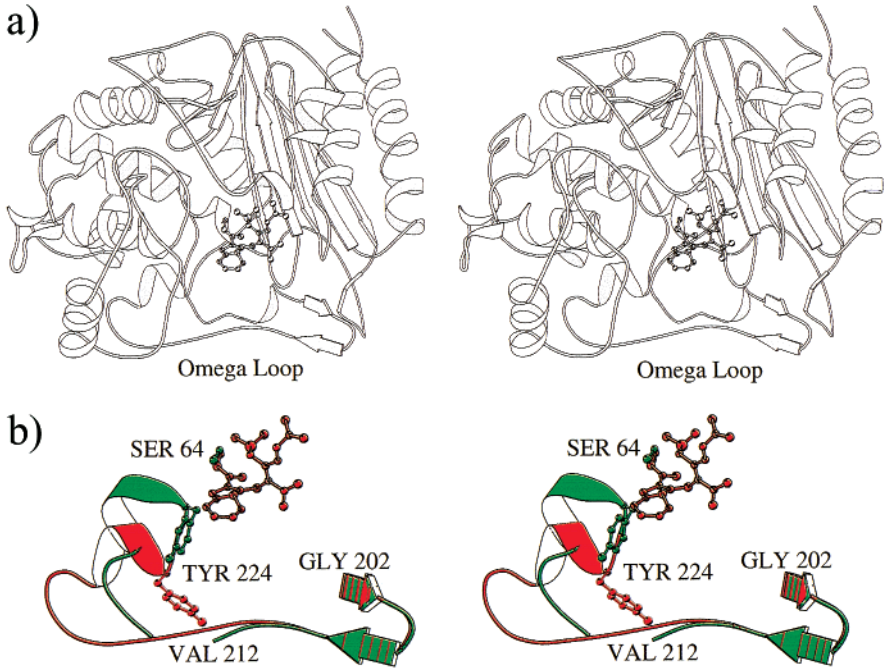

FIGURE 3: (a) MOLSCRIPT (*42*) drawing of the GC1 β-lactamase with intermediate **8** bonded to Ser64. (b) Overlay of Ω-loops in the liganded (red) and unliganded (green) enzyme, showing the intermediate and the movement of Tyr224.

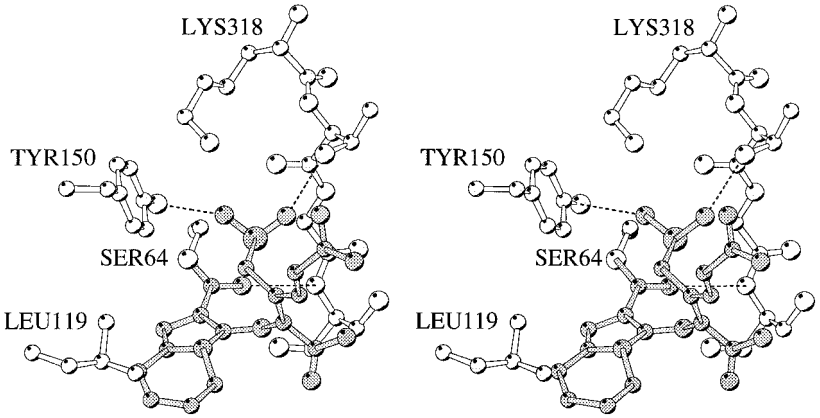

FIGURE 4: Stereoview of intermediate **8** and its environment. Hydrogen bonds are indicated by dashed lines. Only the primary rotamer of the sulfinate anion is drawn. This view angle is similar to that in Figures 2a and 3.

conformation. This, in turn, would allow the six-member cephalosporin ring to remain in a lower position in the binding site such that the C4 carboxylic acid group does not block the deacylationg water molecule, and a faster deacylation rate is restored. This movement of the Ω-loop provides an explanation for the much increased k_{cat} of the GC1 enzyme relative to the P99 enzyme in the hydrolysis of ceftazidime (*12*).

Design of the Sulfone Inhibitor. Although β-lactamase inhibitors derived from the penam, penem, and clavam skeleton are well-known, the 7-alkylidenecephalosporin sulfones (**2**) represent the first potent cephalosporin-derived inhibitors (*19*). Our initial reports of these sulfones described examples with selective class C β-lactamase inhibitory activity and others with selective class A inhibitory activity but none having the highly desirable ability to inhibit both class A and class C enzymes. In particular, the first 7-(heteroaryl)alkylidenecephems could only inhibit the class C cephalosporinases. However, the recently reported DVR-II-41S (**3**) was designed with 3′-unsaturation (*21*), similar to that of the known β-lactamase substrate, nitrocefin. Since nitrocefin is an excellent substrate of nearly all classes of β-lactamase, we hoped that such a modification would improve recognition by several classes of the enzyme. Gratifyingly, this new 7-(heteroaryl)alkylidene cephem, along with a number of other 3′-unsaturated cephalosporin sulfones, was observed to display outstanding inhibition of both class A and class C β-lactamases, including the extended-spectrum class C GC1 β-lactamase, described here.

Interaction between the Intermediate and Enzyme. The enzymic environment of the Ser64-bound intermediate is shown in Figure 4. The oxygen atom of the β-lactamyl carbonyl group forms a linear hydrogen bond to the backbone amide of Ser321 (3.0 Å). This oxygen atom is within 2.8 Å of the amide of Ser64, but the nearly 90° N···OC angle is not optimum for hydrogen bonding. This imperfection in hydrogen bonding will reduce polarization of the carbonyl bond, decrease stabilization of an oxyanion species, and increase instead the resonance stabilization of the acyl intermediate, as discussed below.

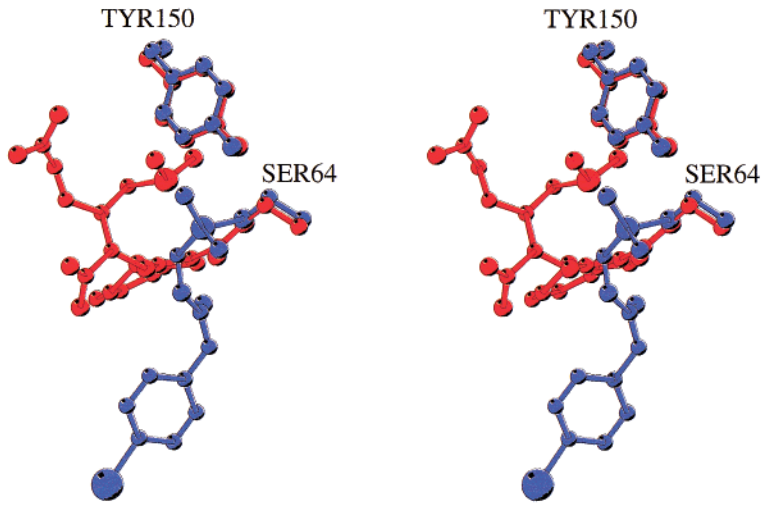

FIGURE 5: Overlay of the acyl intermediate **8** in the GC1 β-lactamase (red) with a phosphonate analogue of the tetrahedral transition state (blue) in the parental P99 β-lactamase [1BLS (*32*)].

The intermediate has one other significant contact with the enzyme. The sulfinate anion is drawn to the vicinity of the cationic Lys318 ammonium group and held not only electrostatically (3.1 Å) but also with strong hydrogen bonds to the hydroxyl groups of Tyr150 (2.7 Å), Thr319 (2.9 Å), and Ser321 via water 557. (With the acyl carbonyl group anchored in the oxyanion hole, the C4 carboxylate of the intermediate is unable to form these favorable interactions.) As a consequence, the positioning of both the carboxylate group and the C3′ amide group is dependent on the positioning of the sulfinate anion, and the carboxylate and acylamide are found to have only weak interactions with the enzyme. Instead, they are hydrated with a few water molecules. For similar reasons, the amide group at N5 is unable to bind to the enzyme. Though the N5 atom is 2.8 Å from the oxygen atom of the acylserine carbonyl group, poor geometry does not permit a strong intramolecular hydrogen bond.

The only remaining interaction between the intermediate and the enzyme is a hydrophobic one involving the aromatic pyridyl system and the side chain of Leu119. The nearby polar side chain of Gln120 is confounded by the edge of the aromatic rings and is observed to be disordered.

The Intermediate's Stability to Hydrolysis: Chemical and Structural Contributions. Figure 1 shows a proposed mechanism for the conversion of DVR-II-41S to the stabilized acyl form observed here. After acylation of the reactive Ser64 is an opening of the dihydrothiazine ring, with ejection of the sulfinate leaving group. Although an analogous ring opening of the five-membered thiazolidine dioxide ring system of the penicillin sulfones (such as sulbactam and tazobactam) is well established (*34*−*36*), this is the first example of such an opening of the six-membered dihydrothiazine dioxide ring of the cephalosporin sulfones. Two factors may favor such an opening in this case: (1) the absence of the more common cephalosporin 3′-acetoxymethyl group which, in the case of many cephalosporin antibiotics, readily loses acetate, leading to an exocyclic methylidenethiazine, and (2) the ability of the 7′-position pyridine nitrogen to provide anchimeric assistance to the departing sulfinate. Indeed, the crystal structure shows that the pyridyl nitrogen becomes bonded to the former C6, implying that the pyridyl nitrogen either assisted the departure of the sulfinate or intercepted the resultant imine as shown. Regardless of the sequence of events, the intermediate **6** loses a proton from the C6 atom, an event possibly assisted by Tyr150 acting as a general base (*32*, *37*). Rearrangement in **6** leads to the aromatic indolizine ring of **7**. During the reaction, the electrostatics of the binding site causes a rotation of the side chain around C4−N5 to produce the observed conformation of intermediate **8**. The ester carbonyl of the acyl intermediate would now be expected to be stabilized toward hydrolysis through favorable resonance interactions with the bicyclic aromatic system, with the indolizine nitrogen, and with the (former) N5 of the cephalosporin (*22*).

Some authors (*33*, *38*, *39*) have discussed whether the N5 nitrogen atom might function as a general base in a substrate-assisted mechanism for the hydrolysis of (nonsulfone) β-lactam intermediates, similar to **4**. In such cases, rotation about the C6−C7 bond might allow N5 to bind and activate the attacking water molecule. However, this role for N5 in the DVR-II inhibitor is not likely. Ring fusion and the planarity of the N5−C6═C7−C═O system in intermediates **6**−**8** would severely restrict conformational mobility. This planar structure would prevent interaction of N5 with a hydrolytic water molecule and at the same time reduce the basicity of the nitrogen (enhancing the stability of the carbonyl group) due to resonance interactions.

Another factor which clearly contributes to the stability of intermediate **8** is structural in nature rather than chemical. A funnel-shaped cluster of five to six water molecules extends from the surface of the enzyme to the sulfinate anion, which effectively separates the water cluster from the acylserine ester carbonyl. It appears that the sulfinate anion, securely anchored by electrostatic and hydrogen bonds, is very well positioned to prevent a water molecule from attacking the external face of the acylserine bond to deacylate the enzyme via the tetrahedral transition state intermediate. A similar proposal was made to explain the stability of bridged monobactam inhibitors containing a sulfonic anion (*40*).

Comparison with a Tetrahedral Transition State Analogue. An overlay of the acyl intermediate **8** with the phosphonate analogue of the tetrahedral transition state for deacylation

in the parental P99 β-lactamase (*32*) is shown in Figure 5. The sulfinate group of **8** lies between the virtual tetrahedral center and the oxygen atom of Tyr150, a residue thought to have a low pK_a and functioning as a general base in deacylation in class C β-lactamases (*32*, *33*, *37*, *41*). The position of the Tyr150 side chain is equivalent in both complexes. Hydrogen bonding of the oxygen atom of Tyr150 to the negative sulfinate group confirms that the tyrosine has become protonated in the inhibition reaction. On the basis of the overlay with the tetrahedral analogue, the sulfinate group would be very close (within 1.2 Å) to the oxygen atom derived from the hydrolytic water molecule, supporting the hypothesis that the sulfinate anion is able to block a water molecule attacking from the external or β-face of the acyl intermediate. Therefore, this protective conformation of the acyl intermediate and the resonance stabilization discussed above are major contributors to the sulfone's long-lived inhibition of class C β-lactamases.

ACKNOWLEDGMENT

This work is based upon data collected at the Cornell High Energy Synchrotron Source (CHESS), which is supported by the NSF under award DMR-9311772, using the Macromolecular Diffraction facility (MacCHESS), which is supported by award RR-01646 from the NIH. We thank Alexandre Kuzin and Paul Moews for computational assistance.

REFERENCES

1. Kotra, L. P., and Mobashery, S. (1998) *Bull. Inst. Pasteur 96*, 139−150.
2. Matagne, A., Dubus, A., Galleni, M., and Frere, J.-M. (1999) *Nat. Prod. Rep. 16*, 1−19.
3. Pares, S., Mouz, N., Petillot, Y., Hakenbeck, R., and Dideberg, O. (1996) *Nat. Struct. Biol. 3*, 284−289.
4. Anderson, J. W., and Pratt, R. F. (2000) *Biochemistry 39*, 12200−12209.
5. Davies, C., White, S. W., and Nicholas, R. A. (2001) *J. Biol. Chem. 276*, 616−623.
6. Knox, J. R., Moews, P. C., and Frere, J.-M. (1996) *Chem. Biol. 3*, 937−947.
7. Galleni, M., Amicosante, G., and Frere, J.-M. (1988) *Biochem. J. 255*, 123−129.
8. Trepanier, S., Knox, J. R., Clairoux, N., Sanschagrin, F., Levesque, R. C., and Huletsky, A. (1999) *Antimicrob. Agents Chemother. 43*, 543−548.
9. Knox, J. R. (1995) *Antimicrob. Agents Chemother. 39*, 2593−2601.
10. Nukaga, M., Haruta, S., Tanimoto, K., Kogure, K., Taniguchi, K., Tamaki, M., and Sawai, T. (1995) *J. Biol. Chem. 270*, 5729−5735.
11. Lobkovsky, E., Moews, P. C., Liu, H., Zhao, H., Frere, J.-M., and Knox, J. R. (1993) *Proc. Natl. Acad. Sci. U.S.A. 90*, 11257−11261.
12. Nukaga, M., Taniguchi, K., Washio, Y., and Sawai, T. (1998) *Biochemistry 37*, 10461−10468.
13. Crichlow, G. V., Kuzin, A. P., Nukaga, M., Sawai, T., and Knox, J. R. (1999) *Biochemistry 38*, 10256−10261.
14. Page, M. I., and Laws, A. P. (1998) *Chem. Commun.*, 1609−1617.
15. Page, M. G. P. (2000) *Drug Resist. Updates 3*, 109−125.
16. Chen, Y. L., Chang, C. W., Hedberg, K., Guarino, K., Welch, W. M., Kiessling, L., Retsema, J. A., Haskell, S. L., Anderson, M., Manousos, M., and Barrett, J. F. (1987) *J. Antibiot. 40*, 803−822.
17. Buynak, J. D., Geng, B., Bachmann, B., and Hua, L. (1995) *Bioorg. Med. Chem. Lett. 5*, 1513−1518.
18. Buynak, J. D., Rao, A. S., Doppalapudi, V. R., Adam, G., and Nidamarthy, S. D. (1999) *Bioorg. Med. Chem. Lett. 9*, 1997−2002.
19. Buynak, J. D., Wu, K., Bachmann, B., Khasnis, D., Hua, L., Nguyen, H. K., and Carver, C. L. (1995) *J. Med. Chem. 38*, 1022−1034.
20. Buynak, J. D., Doppalapudi, V. R., Rao, A. S., Nidamarthy, S. D., and Adam, G. (2000) *Bioorg. Med. Chem. Lett. 10*, 847−851.
21. Buynak, J. D., Doppalapudi, V. R., and Adam, G. (2000) *Bioorg. Med. Chem. Lett. 10*, 853−857.
22. Chen, Y. L., Chang, C. W., and Hedberg, K. (1986) *Tetrahedron Lett. 27*, 3449−3452.
23. Nukaga, M., Tsukamoto, K., Yamaguchi, H., and Sawai, T. (1994) *Antimicrob. Agents Chemother. 38*, 1374−1377.
24. Otwinowski, Z., and Minor, W. (1997) *Methods Enzymol. 276*, 307−326.
25. Navaza, J. (1994) *Acta Crystallogr. A50*, 157−163.
26. Kabsch, W. (1976) *Acta Crystallogr. A32*, 922−923.
27. Brunger, A. T. (1992) *X-PLOR: A system for X-ray crystallography and NMR*, Yale University Press, New Haven, CT.
28. Brunger, A. T. (1992) *Nature 355*, 472−475.
29. Sack, J. S. (1988) *J. Mol. Graphics 6*, 224−225.
30. Brunger, A. T., Adams, P. D., Clove, G. M., Delano, W. L., Gros, P., Grosse-Kunstleve, R. W., Jiang, J.-S., Kuszewski, J., Nilges, M., Pannu, N. S., Read, R. J., Rice, L. M., Simonson, T., and Warren, G. L. (1998) *Acta Crystallogr. D54*, 905−921.
31. Tranier, S., Bouthors, A.-T., Maveyraud, L., Guillet, V., Sougakoff, W., and Samama, J.-P. (2000) *J. Biol. Chem. 36*, 28075−28082.
32. Lobkovsky, E., Billings, E. M., Moews, P. C., Rahil, J., Pratt, R. F., and Knox, J. R. (1994) *Biochemistry 33*, 6762−6772.
33. Patera, A., Blaszczak, L. C., and Shoichet, B. K. (2000) *J. Am. Chem. Soc. 122*, 10504−10512.
34. Knowles, J. R. (1985) *Acc. Chem. Res. 18*, 97−104.
35. Imtiaz, U., Billings, E. M., Knox, J. R., and Mobashery, S. (1994) *Biochemistry 33*, 5728−5738.
36. Kuzin, A. P., Nukaga, M., Nukaga, Y., Hujer, A. M., Bonomo, R. A., and Knox, J. R. (2001) *Biochemistry 40*, 1861−1866.
37. Oefner, C., D'Arcy, A., Daly, J. J., Gubernator, K., Charnas, R. L., Heinze, I., Hubschwerfen, C., and Winkler, F. K. (1990) *Nature 343*, 284−288.
38. Ishiguro, M., and Imajo, S. (1996) *J. Med. Chem. 39*, 2207−2218.
39. Bulychev, A., Massova, I., Miyashita, K., and Mobashery, S. (1997) *J. Am. Chem. Soc. 119*, 7619−7625.
40. Heinze-Krauss, I., Angehrn, P., Charnas, R. L., Gubernator, K., Gutknecht, E. M., Hubschwerlen, C., Kania, M., Oefner, C., Page, M. G. P., Sogabe, S., Specklin, J.-L., and Winkler, F. K. (1998) *J. Med. Chem. 41*, 3961−3971.
41. Lamotte-Brasseur, J., Dubus, A., and Wade, R. C. (2000) *Proteins: Struct., Funct., Genet. 40*, 23−28.
42. Kraulis, P. (1991) *J. Appl. Crystallogr. 24*, 946−950.

BI010131S